https://doi.org/10.1016/j.nanoen.2022.107382

Flexible Modulations on Selectivity of Syngas Formation via CO_2 Reduction on Atomic Catalysts

Mingzi Sun[1], Bolong Huang[1,2,3,4,]*

[1]Department of Applied Biology and Chemical Technology, The Hong Kong Polytechnic University, Hung Hom, Kowloon, Hong Kong SAR, China
[2]Beijing Institute of Nanoenergy and Nanosystems, Chinese Academy of Sciences, Beijing 100083, China
[3]Research Institute for Smart Energy (RISE), The Hong Kong Polytechnic University, Hung Hom, Kowloon, Hong Kong SAR, China
[4]Research Institute for Intelligent Wearable Systems (RI-IWEAR), The Hong Kong Polytechnic University, Hung Hom, Kowloon, Hong Kong SAR, China

*Corresponding author. Email: bhuang@polyu.edu.hk

Abstract

Electrocatalysts with multi-active sites are significant to achieve the flexible selectivity modulation of syngas components to couple with different chemical productions. Compared to the complicated composite electrocatalyst to realize multi-active sites, Graphdiyne (GDY) based single atomic catalysts (SACs) have offered a simple approach through intrinsic electroactivity of the GDY and the variation of atomically dispersed metal. In this work, we have proposed a systematic investigation of syngas formation on the GDY-SACs. It is found that f and p orbitals of lanthanide and GDY are able to facilitate the adsorption of reactants CO_2 and H_2O, respectively, which flexibly control the CO: H_2 ratios in syngas formation. Machine learning results indicate that solely relying on the adsorption energies leads to deviated selectivity. This indicates that a comprehensive understanding of thermodynamic preference and electronic structures is needed to achieve the highly accurate prediction of selectivity. This work has supplied an innovative understanding of the selectivity control in syngas formation, which benefits the future rational design of atomic catalysts for efficient CO_2 reduction.

Keywords: Syngas Formation, CO_2 Reduction, Atomic Catalyst, Selectivity, Graphdiyne

Introduction

Electrochemical CO_2 reduction reactions (CO_2RR) towards different high-valued chemicals have become the critical method to the carbon capture, utilization, and storage technologies as well as the carbon-neutral cycle[1-5]. Owing to the competitive hydrogen evolution reaction (HER), the CO_2RR process often meets the challenges of low Faradic efficiency and poor selectivity. However, rather than prohibiting the competitive HER process, integrating CO_2RR and HER to synthesis syngas with tunable CO/H_2 ratio is promising for industrial applications [6-7]. Therefore, the electrocatalytic production of syngas from the simultaneous reduction of CO_2 and H_2O has become a promising technology[8]. Different CO/H_2 ratios in the syngas can meet the requirements of varied chemical products: $CO/H_2 = 1:2$ for methanol synthesis and Fischer-Tropsch reactions, $CO/H_2 = 1-3.33$ for syngas fermentation, $CO/H_2 = 1:1$ for dimethyl ether [9-10]. Owing to the relatively low Faradaic efficiency (FE) and selectivity of direct CO_2RR to methanol or other liquid products and the complicated separation of final products, the electrosynthesis of syngas becomes highly attractive due to their broad applications for chemical and aerospace industrials. It is necessary to develop electrocatalysts that can produce a flexible CO/H_2 ratio with high syngas yield. Although noble metals such as Pd, Cu, Au have shown high performances in the synthesis of hydrocarbons, their high cost and low abundance limit the large applications for chemical industries[11-13]. Most importantly, the flexible modulations of CO/H_2 are still very challenging for these catalysts.

Single atomic catalysts (SAC) show the feature with atomically dispersed metal atoms on the support surface, which shows the merits of 100% utilization of the metal atoms, the well-defined active sites, and tunable coordination environments[14-15]. Compared to the conventional nanocatalysts, the much-reduced loading of metals in ACs is able to achieve even better performances, which significantly lowers the cost of electrocatalysts in practical applications[16-21]. Since there are two reactions involved in the synthesis of the syngas, SAC has become the most promising method to realize multi-active sites for the modulations of the H_2:CO ratio[22-24]. More importantly, the coupling between support and atomically dispersed metal sites becomes a more effective method to modulate the H_2:CO ratio[25]. SAC with dual active sites are particularly attractive electrocatalysts for the synthesis of syngas since the electroactivity towards both CO_2RR and HER can be individually tuned by modulations of metals and concentrations[26-28]. Lin et al. have reported the anchoring of both Ni nanoparticles and single Ni atoms on mesoporous nitrogen-carbon nanorods, which display high selectivity and electroactivity in the reduction of H_2O and CO_2, respectively [22-23]. A similar strategy has been also reported in Co-based AC by Amal and coworkers on the synthesis of Co single-atom-decorated N-doped graphitic carbon shell-encapsulated cobalt nanoparticle [24]. This work has tuned the H_2/CO ratio from 0.5 to 1.5 over a broad range of potential from -0.5 V to -0.8 V vs RHE. Besides the combination with the nanoparticle, the functional groups from support can also facilitate syngas formation. Jiang and Li have utilized the N functional groups and the single Co sites as active sites for CO_2RR and HER, respectively, realizing the CO/H_2 ratio at 2:1 with near 100% faradic efficiency[25]. The dual atomic catalysts (DAC) are particularly attractive electrocatalysts for the synthesis of syngas since the electroactivity towards both CO_2RR and HER can be individually tuned by the modulations of metals and concentrations[26]. Chen et al. reported that the Co-Ni embedded on N-doped carbon shows a high syngas yield (total current density > 74 mA cm^{-2} with tunable CO/H_2 ratios (0.23~3.26), which is suitable for further coupling with other industrial catalytic reactions[27]. However, it is noted that all the SAC or DAC are still limited to a few transition metals (i.e. Ni, Co) while the potentials of other metals still require more in-depth explorations. Due to the intrinsic electroactivity of graphdiyne (GDY) towards the HER[29], the GDY-based SACs have possessed great potential in the CO_2 reduction towards the syngas formation, which has rarely been studied.

In this work, we have revealed reveal the electroactivity and selectivity of GDY-SAC for syngas formation. GDY-Ln SAC has been screened out as promising candidates to reach syngas formation with flexible modulations of CO/H_2 ratios, which relies on the orbital coupling effect of metals and GDY to control the CO_2RR and HER, respectively. The probing of selectivity for the syngas requires the integration of thermodynamic energies and electronic structures. Most importantly, understanding the structure-property correlation through the ideal platform GDY-SAC benefits the design and search of novel SACs with high performances in the synthesis of syngas.

Selectivity of CO and H_2

For the GDY-SAC, we focus on the selectivity of the metal sites and the neighboring two carbon sites on the alkyl chain (C1 and C2) by explorations of transition metals (TMs) and lanthanide (Ln) (Figure S1). To reveal the selectivity of CO_2RR and HER, we have compared the adsorption energies of CO_2 and H_2O since the alkaline environment is usually favored (**Figure 1**). Notably, the selectivity towards H_2 is stronger than CO due to the lowered adsorption energies. For 3d-TMs based GDY-SACs, the metal sites will be prone to the HER rather than the reduction of CO_2 (**Figure 1a**). We notice that the C1 site on some 3d-TMs based GDY-SACs shows the preferred formation of CO, which is induced by the large energy barrier for the formation of H_2[30]. Similarly, in the alkyl chains of 4d-TMs based GDY-ACs, the metal sites mostly facilitate the CO_2RR while the carbon sites are element-dependent on the selectivity towards CO_2RR and HER, indicating the existence of multi-active sites in GDY-based ACs (**Figure 1b**). This leads to the possibility of CO: H_2 ratio by the modulation of metal loading during the synthesis of SACs. However, the formation of CO becomes preferred on GDY-5d SACs when compared to 3d and 4d-TMs based GDY-SACs (**Figure 1c**). In addition, we notice that the selectivity of both carbon sites and metal sites show a broad distribution of data, leading to the element-dependent selectivity for both CO and H_2 generation. This is distinct from GDY-3d and GDY-4d SACs, where the metal sites facilitate the CO formation while the alkyl chains of GDY prefer the H_2 formation. This indicates that the role of metal and carbon sites in the dual active sites for syngas may show variations. To realize the coupling with the industrial synthesis, 3d and 4d-TMs based GDY-SACs are promising candidates since they are more possible to increase the concentrations of H_2 in the syngas formation, enabling more potential applications. In the meantime, GDY-Ln SACs demonstrate the element-dependent trend in the selectivity, which supplies more selections to realize the syngas formation with flexible modulations of the components (**Figure 1d**).

Component Modulations in Syngas

To comprehensively evaluate the selectivity of syngas, we have mapped out the reaction energy of syngas formation with different H_2:CO ratios. For the 1:1 H_2:CO ratio, the early TMs based GDY-SACs are more energetically favorable than those late TMs based GDY-SACs, which are different from the selectivity comparison by adsorption energies (**Figure 2a**). This is attributed to the larger barrier from the chemisorption of proton than the combination with CO_2. With the increasing concentration of H_2 in the syngas, the distinct reaction trends between early and late TMs (**Figure 2b**). Such a trend still remains even for the 3:1 ratio of H_2:CO (**Figure 2c**). Based on the reaction energies and the selectivity, the early 3d and 4d TMs based GDY-SACs are potential candidates to achieve the flexible control of syngas components. Meanwhile, we notice that the reaction trend of GDY-Ln SACs is not strongly affected by the H_2 concentration in the syngas. Although GDY-Sm and GDY-Eu have been proven with strong HER potential[30], the large energy barriers of syngas formation are ascribed to the sluggish CO_2RR reactions. Thus, it is summarized that the early and late GDY-Ln SACs are promising candidates due to the smaller energy barriers at the initial dissociation of H_2O. Through these results, the simple adsorption energy comparison cannot reveal the selectivity of syngas, where the energetic trends should always be considered for the understanding of selectivity.

Correlation with Electronic Structures

The adsorptions of key reactants are a significant factor in affecting the syngas formation, which is usually determined by the orbital coupling. On the atomic catalysts, the electronic structures of many supports such as carbon materials and oxide usually have strong contributions from the p-orbitals of carbon skeletons. However, the p-band centers of these materials have rarely been discussed in previous works. Considering the strong interactions between the support and anchoring metals, the p-band center is a highly important factor in modulating the electronic structures as well as the electroactivity for SAC. In particular, our previous work has illustrated the strong (*sp*)-*d* overlapping for Ni on GDY, leading to extrinsic charge compensation and the formation of zero-valence [29].Therefore, both d-band centers of metal and p-band centers of GDY as well as their correlations with the adsorption energies are investigated.

For CO_2 adsorption on the metal site, it is noted that the d-band center of TMs is correlated with the adsorption energies at a limited level (**Figure 3a**). In comparison, from Ce to Er, the f-band center demonstrates a similar trend with the adsorption energies of CO_2, indicating the significant role of *f* electrons. As the *f* orbitals become fully occupied, the influences of electronic structures become much weaker, leading to less correlations with the adsorption of CO_2. These results demonstrate the significant contributions of *p-f* orbital coupling in promoting syngas formation. This is consistent with our previous works that lanthanide elements are able to achieve the efficient *f-d* couplings to realize the self-balance effect to improve the electroactivity [31]. In addition, the p-band center has been proved that can be effectively modulated by the anchoring elements on GDY [32-33]. Accordingly, we notice a distinct trend of H_2O adsorption, where the p-band centers of the carbon sites are strongly correlated with the adsorption energies (**Figure 3b**). This trend is applicable for all the transition metals based GDY-SACs, indicating a promising descriptor or criteria to predict the adsorption trends for H_2O on GDY-SAC. In comparison, such correlation is absent in the GDY-Ln SACs, supporting that the p-band center determines the adsorption of H_2O. This important correlation will become a highly useful reference for identifying potential electrocatalysts candidates for syngas, HER, or other electrochemical reactions. The correlation between the d-band center and adsorption energies mostly followed the trend of the d-band center (**Figure 3c**). This indicates that the adsorption of CO_2 shows limited influences on the modulations of the d-band center, which is determined by the interactions between metal and GDY. In addition, the p-d band center difference shows an evident linear correlation (**Figure 3d**). In comparison, the variations of H_2O adsorption energies show a weaker correlation with the p-d band canter difference than that of the p-band center. The involvements of the d orbitals result in less regulated adsorption behaviors. These results demonstrate that different electronic structures modulate different preferences of reactants, which supplies critical references to find the appropriate ACs to reach the flexible control of syngas components.

Predictions of Selectivity by Machine Learning

Compared to many of today's state-of-the-art machine learning (ML) models Gaussian Process Regression (GPR) is a remarkably powerful class of ML algorithms, which only relies on a few parameters to make reliable predictions. Another advantage is that since GPR is a non-parametric method, it can be applied effectively to solve a wide variety of supervised learning problems, even when the dataset is relatively small, which is highly suitable for our work. Compared to other supervised learning algorithms, GPR estimates both expected values and uncertainty, which is especially beneficial for decision-making systems to achieve more realistic predictions. The disadvantage of GPR is that it is not sparse, which means that it uses the whole samples/features information to perform the prediction. This will lead to the lower efficiency of predictions in high dimensional spaces, especially when the number of features exceeds a few dozen. However, in our work, this limitation can be avoided since we did not input too many features as the parameters for prediction. Therefore, in this work, the GPR method has been applied for the ML predictions. As a parallel theoretical exploration, the selectivity of syngas on the metal sites of GDY-ACs has been predicted regarding the adsorption energies by four different strategies. For the alkaline environment, we notice that H_2 is slightly more preferred than the CO, which is consistent with our theoretical calculations (**Figure 4a**). Notably, Ce, Er, Dy based GDY-ACs have been predicted with strong potential to increase the CO concentration in syngas. Meanwhile, for the acidic environment, it is found that the concentration of syngas becomes more modulatable due to widely distributed adsorption energies (**Figure 4b**). These results confirm that the selectivity is also potentially affected by the electrolyte of CO_2RR. The selectivity is also investigated by the direct comparison of formation energies on CO and H_2 (**Figure 4c**). Interestingly, the CO formation energies are mostly lower than that of H_2, supporting a stronger formation trend of the CO, supporting that CO has been the dominant product for CO_2RR on AC. For another condition, we predict the energy barriers determined by the energy difference between the initial adsorption to the final formation of CO and H_2 (**Figure 4d**). The energy barriers of CO formation on most GDY-ACs are smaller than that of H_2, leading to a higher possibility of CO formation. Through different comparing strategies, we are able to obtain varied selectivity results in the syngas formation from CO_2RR and HER. This indicates that the comprehensive explorations of both thermodynamic adsorptions and electronic modulations are essential references to an insightful understanding of the flexible control of syngas components.

Conclusions

In this work, we have carried out an in-depth exploration of syngas formation on the GDY-based SACs regarding both thermodynamic energies and electronic structures, which demonstrates the multi-active site features in GDY-SACs for CO and H_2 formation. Our results indicate that a comprehensive understanding of selectivity should be investigated by both the initial adsorption preferences and reaction trends from energetic perspectives. Most importantly, it is noted that the f-band center of Ln and p-band center of the alkyl chain plays a key role in the adsorption of CO_2 and H_2O. This proves the multi-active site in GDY-SACs, where the metal sites and GDY facilitate the CO_2RR and HER, respectively. Depending on the revealing of critical factors of selectivity, the selection of appropriate GDY-ACs is able to reach the flexible control of CO: H_2 ratios in the syngas for broad applications.

Competing interests

The authors declare no competing interests.

Acknowledgments

The authors gratefully acknowledge the support from the National Key R&D Program of China (2021YFA1501101), the NSFC/RGC Joint Research Scheme Project (N_PolyU502/21), and the funding for Projects of Strategic Importance of The Hong Kong Polytechnic University (Project Code: 1-ZE2V).

References

[1] H. Zhang; W. Cheng; D. Luan; X. W. Lou, *Angew. Chem. Int. Ed.* **2021,** *60* (24), 13177-13196.

[2] S. Nitopi; E. Bertheussen; S. B. Scott; X. Liu; A. K. Engstfeld; S. Horch; B. Seger; I. E. L. Stephens; K. Chan; C. Hahn; J. K. Norskov; T. F. Jaramillo; I. Chorkendorff, *Chem. Rev.* **2019,** *119* (12), 7610-7672.

[3] S. Liu; J. Xiao; X. F. Lu; J. Wang; X. Wang; X. W. D. Lou, *Angew. Chem. Int. Ed.* **2019,** *58* (25), 8499-8503.

[4] S. Liu; X. F. Lu; J. Xiao; X. Wang; X. W. D. Lou, *Angew. Chem. Int. Ed.* **2019,** *58* (39), 13828-13833.

[5] S. Jin; Z. Hao; K. Zhang; Z. Yan; J. Chen, *Angew. Chem. Int. Ed.* **2021,** *60* (38), 20627-20648.

[6] Z. B. Hoffman; T. S. Gray; K. B. Moraveck; T. B. Gunnoe; G. Zangari, *ACS Catal.* **2017,** *7* (8), 5381-5390.

[7] Q. Chang; J. Kim; J. H. Lee; S. Kattel; J. G. Chen; S. I. Choi; Z. Chen, *Small* **2020,** *16* (49), e2005305.

[8] A. S. Varela, *Nat. Energy* **2021,** *6* (7), 698-699.

[9] M. B. Ross; C. T. Dinh; Y. Li; D. Kim; P. De Luna; E. H. Sargent; P. Yang, *J. Am. Chem. Soc.* **2017,** *139* (27), 9359-9363.

[10] W. Sheng; S. Kattel; S. Yao; B. Yan; Z. Liang; C. J. Hawxhurst; Q. Wu; J. G. Chen, *Energy Environ. Sci.* **2017,** *10* (5), 1180-1185.

[11] B. M. Tackett; J. H. Lee; J. G. Chen, *Acc. Chem. Res.* **2020,** *53* (8), 1535-1544.

[12] F. Marques Mota; D. L. T. Nguyen; J.-E. Lee; H. Piao; J.-H. Choy; Y. J. Hwang; D. H. Kim, *ACS Catal.* **2018,** *8* (5), 4364-4374.

[13] P. Chen; Y. Jiao; Y.-H. Zhu; S.-M. Chen; L. Song; M. Jaroniec; Y. Zheng; S.-Z. Qiao, *J. Mater. Chem. A* **2019,** *7* (13), 7675-7682.

[14] X. F. Yang; A. Wang; B. Qiao; J. Li; J. Liu; T. Zhang, *Acc. Chem. Res.* **2013,** *46* (8), 1740-8.

[15] S. Ji; Y. Chen; X. Wang; Z. Zhang; D. Wang; Y. Li, *Chem. Rev.* **2020**.

[16] C. Zhao; X. Dai; T. Yao; W. Chen; X. Wang; J. Wang; J. Yang; S. Wei; Y. Wu; Y. Li, *J. Am. Chem. Soc* **2017,** *139* (24), 8078-8081.

[17] A. Wang; J. Li; T. Zhang, *Nat. Rev. Chem.* **2018,** *2* (6), 65-81.

[18] S. Ji; Y. Chen; X. Wang; Z. Zhang; D. Wang; Y. Li, *Chem. Rev.* **2020,** *120* (21), 11900-11955.

[19] S. Ding; M. J. Hülsey; J. Pérez-Ramírez; N. Yan, *Joule* **2019,** *3* (12), 2897-2929.

[20] J. Leverett; R. Daiyan; L. Gong; K. Iputera; Z. Tong; J. Qu; Z. Ma; Q. Zhang; S. Cheong; J. Cairney; R. S. Liu; X. Lu; Z. Xia; L. Dai; R. Amal, *ACS Nano* **2021,** *15* (7), 12006-12018.

[21] A. S. Varela; N. Ranjbar Sahraie; J. Steinberg; W. Ju; H.-S. Oh; P. Strasser, *Angew. Chem. Int. Ed.* **2015,** *54* (37), 10758-10762.

[22] X. Wang; X. Sang; C. L. Dong; S. Yao; L. Shuai; J. Lu; B. Yang; Z. Li; L. Lei; M. Qiu; L. Dai; Y. Hou, *Angew. Chem. Int. Ed.* **2021,** *60* (21), 11959-11965.

[23] W. Zhu; J. Fu; J. Liu; Y. Chen; X. Li; K. Huang; Y. Cai; Y. He; Y. Zhou; D. Su; J.-J. Zhu; Y. Lin, *Appl.Catalysis B: Environ.* **2020,** *264*.

[24] R. Daiyan; R. Chen; P. Kumar; N. M. Bedford; J. Qu; J. M. Cairney; X. Lu; R. Amal, *ACS Appl. Mater. Interf.* **2020,** *12* (8), 9307-9315.

[25] X. Song; H. Zhang; Y. Yang; B. Zhang; M. Zuo; X. Cao; J. Sun; C. Lin; X. Li; Z. Jiang, *Adv. Sci.* **2018,** *5* (7), 1800177.

[26] W. Ni; Z. Liu; X. Guo; Y. Zhang; C. Ma; Y. Deng; S. Zhang, *Appl. Catal. B: Environ.* **2021,** *291.*

[27] Q. He; D. Liu; J. H. Lee; Y. Liu; Z. Xie; S. Hwang; S. Kattel; L. Song; J. G. Chen, *Angew. Chem. Int. Ed.* **2020,** *59* (8), 3033-3037.

[28] X. Yang; T. Tat; A. Libanori; J. Cheng; X. Xuan; N. Liu; X. Yang; J. Zhou; A. Nashalian; J. Chen, *Mater. Today* **2021,** *45*, 54-61.

[29] Y. Xue; B. Huang; Y. Yi; Y. Guo; Z. Zuo; Y. Li; Z. Jia; H. Liu; Y. Li, *Nat. Commun.* **2018,** *9* (1), 1460.

[30] M. Sun; A. W. Dougherty; B. Huang; Y. Li; C. H. Yan, *Adv. Energy Mater.* **2020,** *10* (12), 1903949.

[31] M. Sun; T. Wu; A. W. Dougherty; M. Lam; B. Huang; Y. Li; C. H. Yan, *Adv. Energy Mater.* **2021,** *11* (13), 2003796.

[32] M. Sun; H. H. Wong; T. Wu; A. W. Dougherty; B. Huang, *Adv. Energy Mater.* **2021,** *11* (30), 2101404.

[33] M. Sun; H. H. Wong; T. Wu; A. W. Dougherty; B. Huang, *Adv. Energy Mater.***2022,** *12* (14), 2103781.

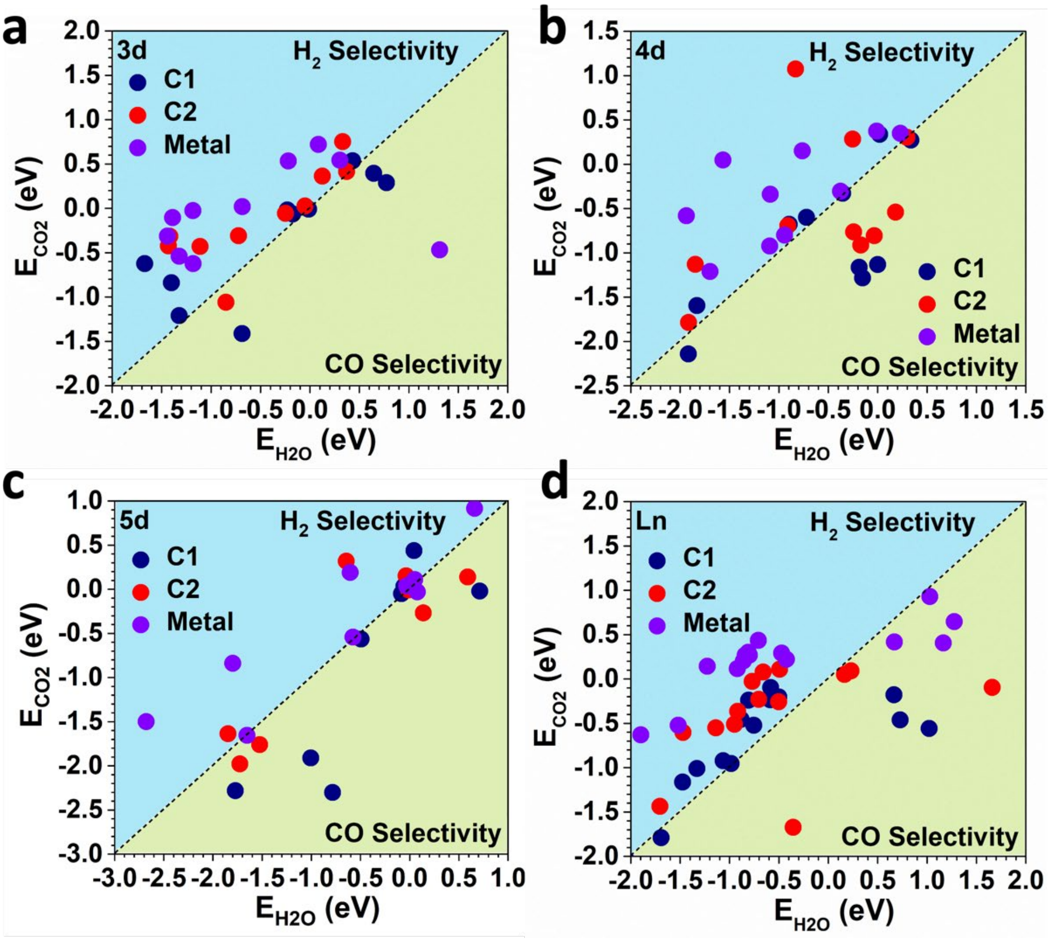

Figure 1. The selectivity comparison of GDY-based SACs with (a) 3d, (b) 4d, (c) 5d TMs and (d) lanthanides.

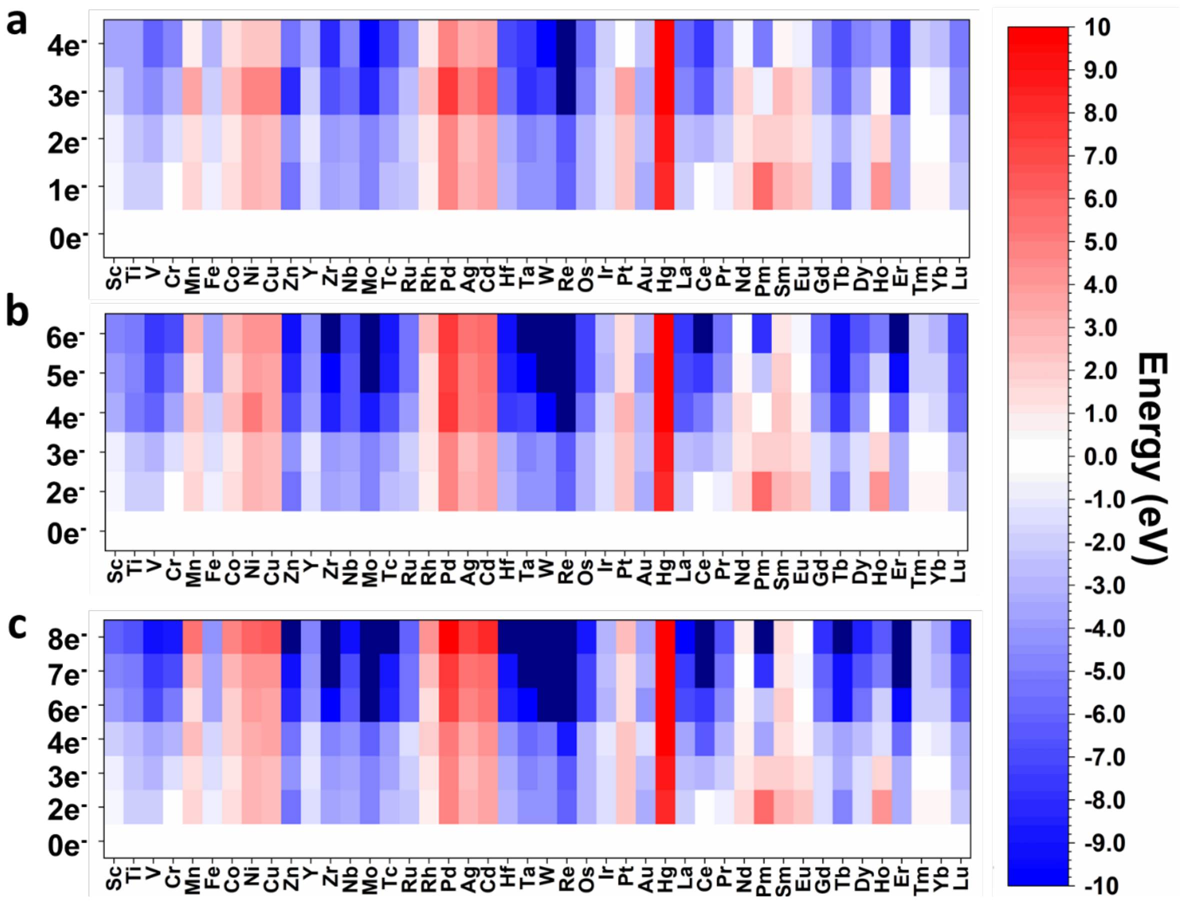

Figure 2. The reaction energy comparison for the syngas formation with H_2:CO ratios of (a) 1:1, (b) 2:1 and (c) 3:1.

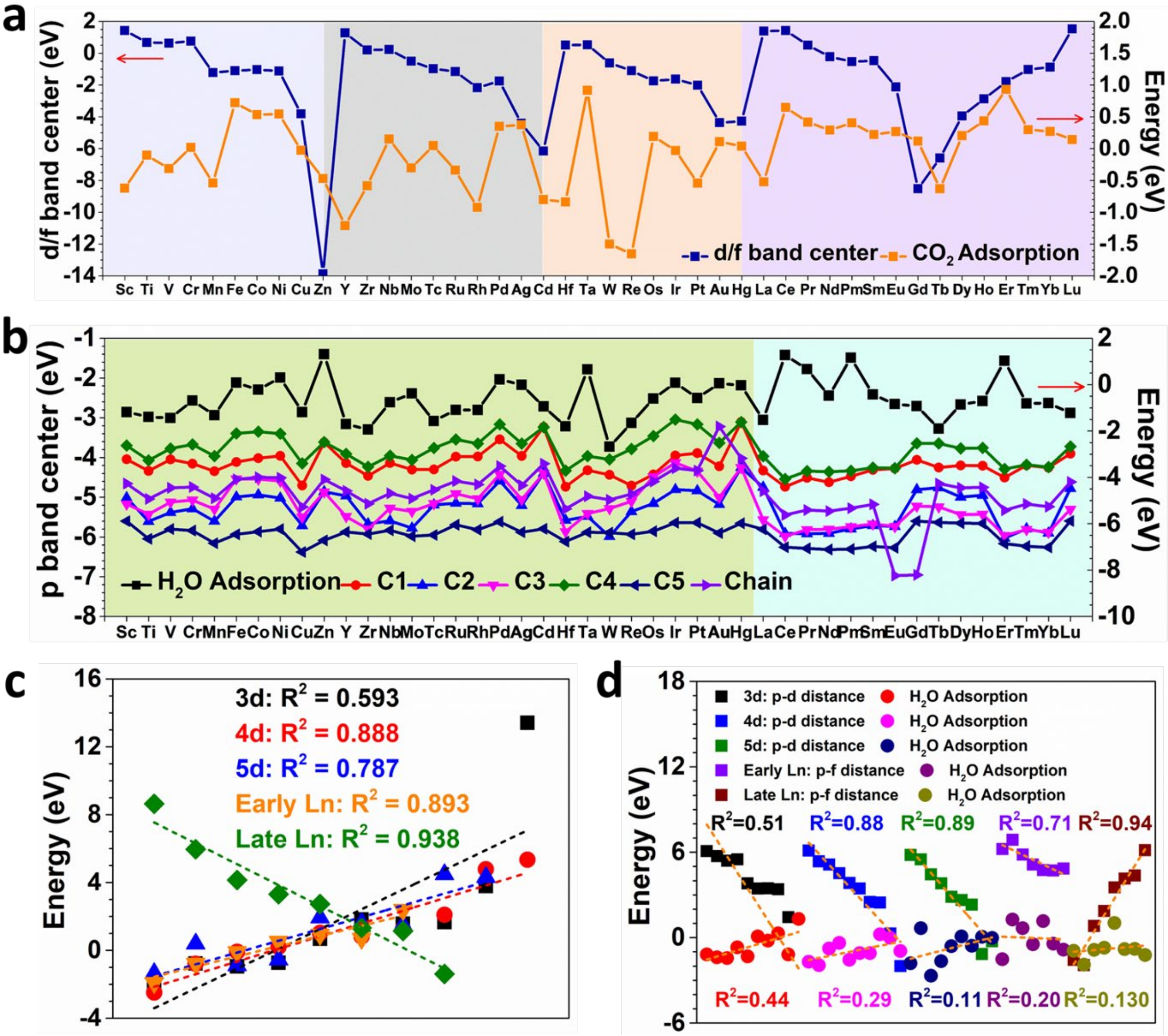

Figure 3. The correlation between electronic structures and the adsorption energies. (a) Adsorption energies of CO_2 with d/f band center. (b) Adsorption energies of H_2O with the p-band center. (c) The influences of CO_2 on the d-band center. (d) Adsorption energies of H_2O with p-d band center difference.

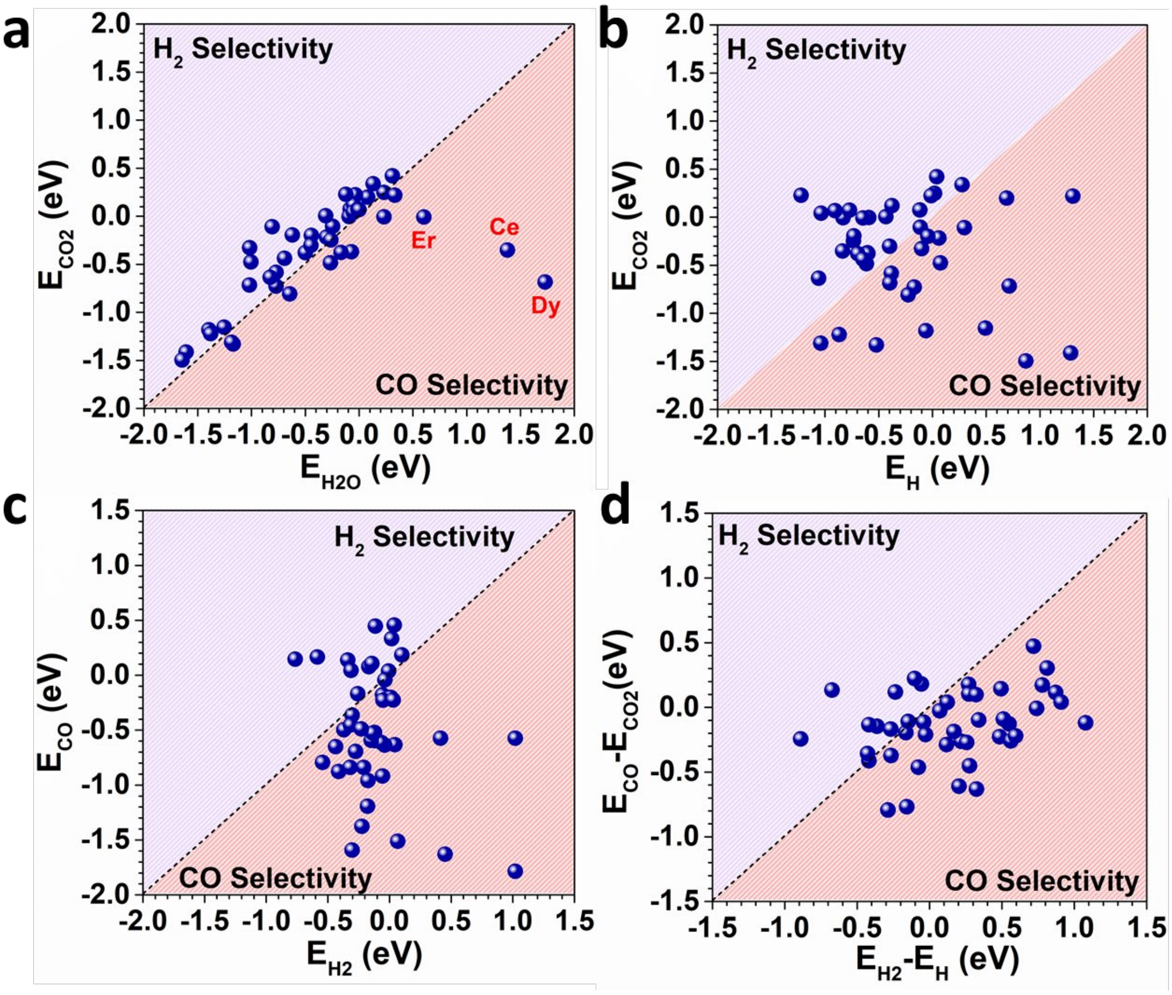

Figure 4. The ML predictions of selectivity in the syngas formation with different approaches. (a) The adsorption energies of CO_2 and H_2O under the alkaline media. (b) The adsorption energies of CO_2 and H under the acidic media. (c) The adsorption energies of CO and H_2. (d) The energy difference between the initial reactants and final products.